Science of the Total Environment 785 (2021) 147289

Contents lists available at ScienceDirect

Science of the Total Environment

journal homepage: www.elsevier.com/locate/scitotenv

Sorption behavior of polycyclic aromatic hydrocarbons on biodegradable polylactic acid and various nondegradable microplastics: Model fitting and mechanism analysis

Maja Lončarski [a], Vesna Gvoić [b,*], Miljana Prica [b], Livija Cveticanin [c], Jasmina Agbaba [a], Aleksandra Tubić [a]

[a] University of Novi Sad, Faculty of Sciences, Department of Chemistry, Biochemistry and Environmental Protection, Trg Dositeja Obradovića 3, 21000 Novi Sad, Serbia
[b] University of Novi Sad, Faculty of Technical Sciences, Department of Graphic Engineering and Design, Trg Dositeja Obradovića 6, 21000 Novi Sad, Serbia
[c] University of Novi Sad, Faculty of Technical Sciences, Department of Mechanics, Trg Dositeja Obradovića 6, 21000 Novi Sad, Serbia

HIGHLIGHTS

- Non-degradable and biodegradable MPs adsorption of so far unexamined PAHs
- Mathematical model developed to investigate mass transfer kinetics of PAHs on MPs
- MPs properties are the most important factor determining adsorption rate of PAHs.
- Adsorption affinity of PLA for PAHs is lower than of non-degradable MPs.

GRAPHICAL ABSTRACT

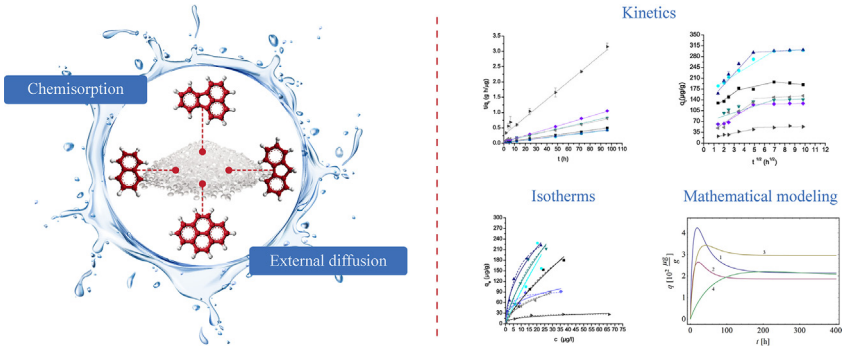

ARTICLE INFO

Article history:
Received 4 January 2021
Received in revised form 16 April 2021
Accepted 16 April 2021
Available online 23 April 2021

Editor: Jay Gan

Keywords:
Microplastics
Biodegradable plastic
Polycyclic aromatic hydrocarbons
Adsorption
Water

ABSTRACT

The main objective of this study was to gain more detailed knowledge of how four selected polycyclic aromatic hydrocarbons (PAHs) interact on six nondegradable types of microplastics (MPs) and one biodegradable plastic (BP) in two water matrices. The results were evaluated using the popular Freundlich and Langmuir isotherm models, as well as a new modified mathematical model. The modified mathematical model was developed to additionally elucidate the adsorption mechanism, to investigate transfer kinetics of PAHs and to predict the variation of adsorption rate and capacity as a function of time. The adsorption kinetics of selected PAHs onto MPs and biodegradable plastic were described best by the pseudo-second order kinetic model ($R^2 = 0.810–0.999$), implying that chemisorption is possibly the adsorption mechanism. The results of the adsorption isotherm study also indicated that adsorption of PAHs on selected types of microplastics was best described by the Langmuir model, implying that adsorption of PAHs is more dominant on powdered types of MPs in both synthetic and real water matrices. On the other hand, the lowest adsorption affinity was achieved for adsorption of PAHs on polylactic acid, indicating that this type of biodegradable plastic would have significantly less impact on the transport and distribution of PAHs through environment.

1. Introduction

Microplastics (MPs), generally defined as plastic particles ranging from 0.1 μm to 5 mm in size, are ubiquitous in water bodies and their widespread occurrence has been reported by a wide range of studies

* Corresponding author.
E-mail address: kecic@uns.ac.rs (V. Gvoić).

https://doi.org/10.1016/j.scitotenv.2021.147289
0048-9697/

(Sørensen et al., 2020; Thompson et al., 2004; C. Wang et al., 2020; Yang et al., 2021). Previous studies have also indicated that in aquatic ecosystems, about 92% of plastics occur in MP form (Kyoung Song et al., 2017). Different studies have reported the negative impact of MPs on the water systems, emphasizing the seriousness of their presence (Chae and An, 2017; Koelmans et al., 2019; Oliveira et al., 2013; Sjollema et al., 2016; Thushari et al., 2017; Zhang et al., 2017).

The available literature data imply that MPs are an ideal adsorbent for polycyclic aromatic hydrocarbons (PAHs) and other environmental pollutants, microorganisms and pathogens, which could serve as carriers allowing them to migrate widely in the natural environment. The negative impact of MPs is also manifested through desorption of contaminants from its surface, resulting in their release into organisms that ingest them (Koelmans et al., 2016; Prunier et al., 2019; Rios Mendoza and Balcer, 2020; Rochman et al., 2013; Rodrigues et al., 2019; Scopetani et al., 2018; T. Wang et al., 2020). Adequate size and specific surface area of MPs are factors that have a major influence on their ingestion speed by organisms and can increase the risk of sorption/desorption of pollutants in water or in the organisms (Bakir et al., 2014; Farrell and Nelson, 2013; Hahladakis et al., 2018; Torres et al., 2021; Wang and Wang, 2018a; Wardrop et al., 2016).

In addition to MPs, the evaluation of biodegradable plastics (BPs) production has resulted in an increasing number of studies of their impact on the environment and human health (Torres et al., 2021). With the increasing interest in everyday use of biodegradable plastic products, it is assumed that their annual production will increase in the next years and the recent widespread use of polylactic acid (PLA) indicates that this type of biopolymer will be one of the most widely used (Weinstein et al., 2020). As is already well known, BPs are designed to degrade completely under controlled conditions. However, there is still a lack of knowledge of their degradation rate in the natural environment. Some studies have also indicated that BPs could act as carriers of different types of environmental pollution and therefore inflict toxic effects similar to conventionally available MPs' on marine organisms (Green et al., 2016; Torres et al., 2021; Zuo et al., 2019).

Two comprehensive literature reviews (Rodrigues et al., 2019; Torres et al., 2021) related to pollutants' interactions with MPs have indicated that the most studied compounds were pesticides (Lončarski et al., 2020; Tubić et al., 2019; F. Wang et al., 2020), PAHs (Avio et al., 2015; Frias et al., 2010; Li et al., 2018a; Liu et al., 2016; Sørensen et al., 2020; Tan et al., 2019; Zhao et al., 2020), polychlorinated biphenyls – PCBs (Devriese et al., 2017) and pharmaceuticals (Fan et al., 2021; Zuo et al., 2019). Among the investigated groups of organic compounds PAHs can be classified as most widely distributed in water ecosystems (Li et al., 2018b; Liu et al., 2016; Sørensen et al., 2020; Tan et al., 2019). They are characterized by low water solubility and a high octanol-water partition coefficient, which results in low bioavailability and a high degree of accumulation in the environment. Due to their high toxicity, mutagenicity and carcinogenic properties, PAHs have been the focus of different scientific studies for many years (Patel et al., 2020; Yu et al., 2019). The European Union Water Framework Directive, US EPA and EU (Directive, 2013; Directive 2000/60/EC, 2000; US EPA, 2014) included 16 PAHs on the list of priority pollutants. Additionally, it has been determined that PAHs' concentrations in rivers can vary between 1.33 ng/L and 1138 μg/L causing serious risk to all water bodies (Mojiri et al., 2019).

Previous studies have provided a wide range of data indicating PAHs' diversity in behavior depending on the experimental conditions (temperature, mixing speed, pH value, ionic strength, salinity, etc.), the physico-chemical properties of investigated MPs (type, surface area, pore size, polarity, functional group, etc.) and the pollutant itself (water solubility, octanol-water partition coefficient, molecular size, acidity, etc.) (Sørensen et al., 2020; Teuten et al., 2016; Wang and Wang, 2018a, 2018b; Zhao et al., 2020; Zuo et al., 2019). However, despite a good number of research papers regarding adsorption behavior of PAHs on MPs such as polyethylene (PE), polystyrene (PS) and polyvinyl chloride (PVC), there is still a lack of information about interactions with other types of MPs which are ubiquitous in the environment, such as polyethylene terephthalate (PET) and polypropylene (PP), as well as with biodegradable plastic materials. Furthermore, based on the available literature, pyrene and phenanthrene are the most commonly used sorbate representatives, resulting in a lack of information on the adsorption behavior of other PAHs on MPs. The largest number of studies regarding adsorption behavior of PAHs onto MPs is conducted in marine-like water matrices. Therefore, the additional knowledge about PAHs' adsorption mechanism on MPs in fresh waters is missing. Additionally, the interactions occurring between PAHs and MPs are typically investigated by two widely used adsorption isotherm models, Freundlich and Langmuir. However, the use of additional models can reveal more detailed information about the adsorption mechanism of PAHs on different types of MPs and BPs. Based on all the above, the aim of this study was to compare adsorption mechanism of PAHs on biodegradable PLA with different types of nondegradable MPs by applying a new mathematical model in addition to well-known adsorption isotherm models. In order to fill in the knowledge gaps findings were attained regarding the adsorption behavior of less studied PAHs (naphthalene, fluorene, and fluoranthene) on various MPs (PP, PET and PE-different sizes and origins) and on PLA as the most widely produced BP. Additionally, the adsorption study was also conducted for pyrene on previously mentioned MPs due to the wide range of published results indicating change in adsorption behavior regarding different factors influencing the adsorption mechanisms.

2. Materials and methods

2.1. Materials

In this study the following MPs were used as adsorbents during the experiment: four types of commercially available MPs – powdered polyethylene standard (PEp, supplied by Thermo Fisher Scientific), granulated polyethylene standard (PEg), polyethylene terephthalate standard (PET) and polypropylene standard (PP) produced by Sigma-Aldrich – two types of powdered polyethylene isolated from different personal care products (PE_PCPs_1 and PE_PCPs_2) and one biodegradable plastic (polylactic acid, PLA), supplied by Sigma Aldrich. Isolation of MPs from personal care products (facial scrubs) – was performed by mixing of the product with boiled water (100 °C) and addition of 30% H_2O_2 for organic matter degradation (Lončarski et al., 2020; Napper et al., 2015; Nuelle et al., 2014).

The sizes of selected powdered types of MPs (Fig. S1) were achieved by scanning electron microscope (TM3030, Hitachi, Japan). These ranged between 80 and 358 μm for the PE particles isolated from the two personal care products, and from 49.7 to 259 μm for PEp (Tubić et al., 2021). The size of the granulated types of selected microplastics (PEg, PET, PP and PLA) was provided by the supplier; in each case, it was 3 mm (Lončarski et al., 2020; Tubić et al., 2019). Characterization of selected commercially available MPs, BPs and particles isolated from personal care products was conducted by Fourier transform infrared spectroscopy (FTIR) (Thermo-Nicolet Nexus 670 FTIR spectrometer, Thermo Fisher Scientific, USA). The attained results of FTIR analysis (Fig. S2) were compared with the Hummel Polymer Sample Library, which confirmed the chemical structure of PEp, PEg, PP, PET and PLA. Based on the FTIR spectra in Fig. S2b and c and a similarity match over 80% with the previously mentioned data library, presence of PE was also confirmed in material isolated from both personal care products. More details about chemical characterization of PE_PCPs_1 and PE_PCPs_2 are given in Lončarski et al. (2020). Physico-chemical properties of investigated MPs attained by Brunner Emmett Teller (BET) analysis are presented in Supplementary material (Table S1).

To establish analytical standards of PAHs, naphthalene, fluorene, fluoranthene and pyrene (Pestanal® Sigma-Aldrich) were used as adsorbates in this study. PAHs' stock solutions with concentrations of 1 mg/mL were prepared in methanol solution. Their physico-chemical properties are presented in Table 1. The selected PAHs differ in

hydrophobicity and water solubility, suggesting that their behavior in the presence of MPs in water would also be different.

Hexane (J.T. Baker), methanol (J.T. Baker), acetic anhydride (Sigma-Aldrich) and hydrogen peroxide (Sigma-Aldrich) were used in the experiments. $CaCl_2$ (Sigma-Aldrich), $NaHCO_3$ (Sigma-Aldrich) and $MgSO_4 \cdot 7H_2O$ (Sigma-Aldrich) were used for preparation of the synthetic water matrix, while HNO_3 (Fluka) and NaOH (Sigma-Aldrich) were used to adjust the pH value of the water. All the reagents were analytical grade without further purification.

2.2. Water matrices

The experiments were conducted in two types of water matrices, synthetic and real. The synthetic water matrix consisted of distilled water enriched with salts, calcium chloride ($CaCl_2$), sodium hydrogen carbonate ($NaHCO_3$) and magnesium sulfate heptahydrate ($MgSO_4 \cdot 7H_2O$). The real water matrix was Danube River water, which was chosen since the river is polluted with plastics. The chemical composition of the synthetic water matrix was similar to the real matrix (Tubić et al., 2019). However, the dissolved organic carbon (DOC) concentration in the synthetic matrix was not adjusted, in order to examine the potential influence on the MPs' adsorption affinity variation towards PAH compounds. The characteristics of the investigated water matrices are presented in Supplementary material (Table S2).

2.3. Batch adsorption experiments

Sorption experiments of adsorption kinetics and adsorption mechanisms of PAHs on various types of MPs were conducted using a batch equilibrium method in laboratory conditions.

2.4. Adsorption kinetic experiments

The adsorption kinetic models were applied to determine the relationship between adsorption time and adsorption capacity, as well as to analyze PAHs' adsorption mechanism on MPs. The Lagergren pseudo-first order kinetic, pseudo second-order kinetic and Weber-Morris models were used in this study (Table S3).

The volume of the water solution was 30 mL for PAH, and the initial concentration of each compound was 100 μg/L. Higher initial concentrations of selected PAHs were used in order to gain improved knowledge of the adsorption mechanism between MPs and PAHs. The mass of powdered MPs (PEp, PE_PCPs_1 and PE_PCPs_2) was 10 mg, and the mass of granulated materials (PEg, PET, PP and PLA) was 20 mg. Complete suspension mixing in the experiments was ensured by using a digital mixer (IKA® Orbital shaker KS 501 Digital), with speed of 150 rpm, at room temperature of 25 °C. All samples were prepared in duplicate. The pH value was 7.23 ± 0.06 for the synthetic water matrix and 7.45 ± 0.07 for the Danube River water. After defined time periods (2, 4, 6, 12, 24, 48, 72 and 96 h), the samples were filtered through a 0.45 μm cellulose acetate membrane filter and then prepared for gas chromatographic (GC) analysis. Physico-chemical characteristics of the synthetic water and Danube River water are given in Tubić et al. (2019) and presented in Supplementary material (Table S2). The adsorption affinity of the tested compounds towards the constituents of the real water matrix was investigated in a set of experiments over 48 h, whereby a change of PAH's concentration was monitored without the presence of MPs in Danube water.

Table 1
Physico-chemical properties of investigated polycyclic aromatic hydrocarbons (Niederer et al., 2007).

Compound	Molecular weight (g/mol)	[a]$\log K_{ow}$	[b]S_w (mg/L)
Naphthalene	128	3.30	31.0
Fluorene	166	4.18	1.69
Fluoranthene	202	5.16	<1
Pyrene	202	4.88	0.135

[a] Octanol-water partition coefficient.
[b] Water solubility.

2.5. Adsorption isotherms experiments

In order to determine the adsorption mechanism of PAHs on MPs, five different initial concentrations of adsorbates were chosen for the experiment (1, 25, 50, 75 and 100 μg/L), while sorbent mass was constant (10 mg for powder and 20 mg for granulated MPs). All experiments were performed at a neutral pH value (7.23 ± 0.06 for the synthetic water matrix and 7.45 ± 0.07 for the Danube River water), while the pH value of the suspension did not change within equilibrium state. After constant stirring for 48 h, the samples were filtered through a cellulose acetate membrane filter, and after adequate preparation analyzed by gas chromatography. The attained results were modeled using five adsorption models: Freundlich, Langmuir, Redlich-Petersen (R-P), Dubinin-Radushkevich (D-R) and Temkin (Table S3).

2.6. Method for mathematical calculation of the mass transfer kinetics

In order to investigate mass transfer kinetics of PAHs on selected MP particles in the synthetic and real water matrices, the predicted variation of the adsorption rate and capacity in time was mathematically considered. The mathematical model was a one-degree-of-freedom differential equation with small nonlinearity and slow time variable parameters. Based on the already published solving procedure for nonlinear equations, an analytical method was introduced (Cveticanin, 2012; Cveticanin, 2014; Cveticanin, 2016). The main assumption of the method was that the mathematical solution of the equation would be the perturbed version of the generating mathematical solution of a linear equation with constant parameters. Thus, first, the closed-form mathematical solution of the linear equation with constant coefficients was calculated. The trial mathematical solution was supposed to have the same form as the generating one, but with slow time arbitrary constants. Hence, the problem was transformed into determination of these constants. After some modification and integration, the approximate solution of the mass transfer kinetic was achieved. The calculated mathematical solution is convenient not only for qualitative but also quantitative interpretation of the mass transfer kinetic.

The model of the sorption rate $\dot{q}$ in time t is given by the following Eq. (1):

$$\dot{q} = k\left(C - \left(\frac{q}{K}\right)^n\right) \tag{1}$$

where $q(t)$ is the sorption capacity, K and n are the Freundlich constants, $C(t)$ is the concentration-time distribution of PAHs in the solution and k is the model constant necessary for unifying of units in the equation. The constant n slightly differs from 1 and the Eq. (1) is with small nonlinearity. Introducing the small parameter $\varepsilon \ll 1$ which satisfies the relation $n = 1 + \varepsilon$, the Eq. (1) transforms into Eq. (2):

$$\dot{q} = \frac{k}{K^{1+\varepsilon}}\left(CK^{1+\varepsilon} - q^{1+\varepsilon}\right) \tag{2}$$

Using the experimental observation, it is seen that the concentration variation is a slow time function. Mathematically, the concentration change is with, so called, 'slow time' which is the product of a constant small parameter ε and time t, i.e., $\tau = \varepsilon t$. Using this assumption, the Eq. (2) is:

$$\dot{q} = \frac{k}{K^{1+\varepsilon}}\left(C(\tau)K^{1+\varepsilon} - q^{1+\varepsilon}\right) \tag{3}$$

The expression (3) is the first order differential equation with slow time variable parameter and small nonlinearity. Unfortunately, there is not a closed form solution for the equation. In this paper an approximate procedure for solving Eq. (3) is introduced (Cveticanin, 2012; Cveticanin, 2014; Cveticanin, 2016). It is based on the similarity of Eq. (3) with the linear differential equation with constant parameters where $\varepsilon = 0$ and $C = C_0 = \text{const.}$

$$\dot{q} = \frac{k}{K}(CK - q) \tag{4}$$

Comparing the Eqs. (3) and (4) it is seen that the Eq. (4) is the perturbed version of Eq. (3). As the perturbation parameter ε is small, it is supposed that the solution of Eq. (3) has to be the perturbed version of the solution of the Eq. (4). The known exact solution of the Eq. (4) is:

$$q = CK\left(1 - \exp\left(-\frac{k}{K}t\right)\right) \tag{5}$$

According to the assumption, the solution of Eq. (3) has to be in the form Eq. (5) but with time variable parameters:

$$q = C(\tau)K\left(1 - \exp\left(-\frac{\mathrm{k}}{\mathrm{K}}\mathrm{t}\right)\right) \tag{6}$$

Substituting the assumed solution Eq. (6) and its time derivative into Eq. (3) it is:

$$\dot{C}(\tau)K\left(1 - \exp\left(-\frac{\mathrm{k}}{\mathrm{K}}\mathrm{t}\right)\right) + Ck\exp\left(-\frac{\mathrm{k}}{\mathrm{K}}\mathrm{t}\right) = \mathrm{k}\left[\mathrm{C} - \mathrm{C}^{1+\varepsilon}\left(1 - \exp\left(-\frac{\mathrm{k}}{\mathrm{K}}\mathrm{t}\right)\right)^{1+\varepsilon}\right] \tag{7}$$

Using the series expansion of the exponential function and after some modification the differential equation of concentration variation yields:

$$\dot{C}(\tau)K = kC\varepsilon\exp\left(-\frac{k}{K}t\right) \tag{8}$$

For the constant value C_0, the concentration time function follows as:

$$C = C_0\, exp\left(\varepsilon\left(1 - \exp\left(-\frac{k}{K}t\right)\right)\right) \tag{9}$$

Analyzing the Eq. (9) it is seen that the concentration variation depends on the ration k/K and the parameter ε. Substituting Eq. (9) into Eq. (6) the approximate relation for external sorption capacity is achieved:

$$q = C_0\, exp\left(\varepsilon\left(1 - \exp\left(-\frac{k}{K}t\right)\right)\right)K\left(1 - \exp\left(-\frac{\mathrm{k}}{\mathrm{K}}\mathrm{t}\right)\right) \tag{10}$$

For $\mathrm{n} = 1 + \varepsilon$ the relation (10) transforms into:

$$q = C_0\, exp\left((n-1)\left(1 - \exp\left(-\frac{k}{K}t\right)\right)\right)K\left(1 - \exp\left(-\frac{\mathrm{k}}{\mathrm{K}}\mathrm{t}\right)\right) \tag{11}$$

Analyzing Eq. (11) it is obvious that the external sorption capacity is increasing from zero to a maximal value $q_{max} = C_0 Kexp((n-1))$. Finally, using Eqs. (3), (9) and (11) the sorption rate is:

$$\dot{q} = kC_0\, exp\left((n-1)\left(1 - \exp\left(-\frac{k}{K}t\right)\right)\right) - k\left(C_0\, exp\left((n-1)\left(1 - \exp\left(-\frac{k}{K}t\right)\right)\right)\right)\left(1 - \exp\left(-\frac{\mathrm{k}}{\mathrm{K}}\mathrm{t}\right)\right)^{\mathrm{n}} \tag{12}$$

The rate is decreasing from a maximal value $\dot{q}_{max} = kC_0$ up to zero. The velocity of decrease depends on k/K and n.

Coefficients of the equations would be obtained from the Freundlich adsorption isotherm experiments, presented in Table S6.

2.7. Analytical procedure, quality assurance and quality control

Determination of the selected PAHs was performed using a gas chromatograph with a mass detector (Agilent 7890A/5975C, GC/MSD) after liquid-liquid extraction with hexane. Sample preparation was performed according to the following steps. 30 mL of the sample was extracted with 3 mL of hexane over 10 min. After extraction, 0.5 mL of the extract was transferred to a vial for GC/MSD analysis with the addition of 2 μL of the internal standard phenanthrene-d10. The chromatography conditions were as follows. The initial oven temperature of 55 °C was held for 1 min, whereby the temperature was increased with a rate of 25 °C/min to 350 °C, where it was held for 3 min. A pulsating splitless injection mode was applied. The injector temperature, the ion source temperature, the quadrupole temperature and the transfer line temperature were 300 °C, 230 °C, 150 °C and 280 °C respectively. Quality parameters data of the applied method for the analysis of residual concentration of PAHs are presented in Table S4.

The pH value of aqueous samples was measured using an instrument 340i, WTW, SenTix®21 electrode, according to the method of SRPS H.Zi.111:1987. Determination of DOC was performed by LiquiTOC II (Elementar, Germany), according to the method SRPS ISO 8245:2007. Determination of chloride concentration in water was performed according to the method SRPS ISO 9297/1:2007. Determination of sulfate concentration was performed by iodometric titration of excess chromate ion with sodium thiosulfate solution after sulfate precipitation by addition of excess barium chromate. Determination of water alkalinity, in a form of hydrogen carbonate concentration, was performed by volumetric method (APHA, 1982).

In order to avoid airborne MPs contamination, all used laboratory glassware and devices were cleaned with ultrapure water before use. Nitrile gloves and cotton clothes were worn in order to reduce contamination from clothes or gloves. Blank tests using ultrapure water instead of water samples were also applied in order to reduce the impact of possible airborne contamination. Additionally, the filters left in a glass Petri dishes for physico-chemical characterization were covered with a protective aluminum case to avoid possible airborne residues and contaminants.

3. Results and discussion

3.1. Adsorption kinetics

Change of the adsorbed amounts of PAHs on MPs (q_t) during time in synthetic water matrix and Danube River water are given in Figs. 1 and 2. The results indicate that the adsorption equilibrium is achieved after 24 h for all investigated PAHs on powdered types of MPs and after 48 h for granulated. Lower equilibrium time required for PAHs adsorption on powdered types of MPs may be due to its significantly higher specific surface area, compared to granulated types (Table S1), which is in line with the results of other authors (Fotopoulou and Karapanagioti, 2012; Wang and Wang, 2018a).

The results attained for adsorption of PAHs on powdered and granulated PE indicated that particle size and specific surface of MPs (Table S1) are important factors which affect its adsorption affinity. It was found that powdered types of PE, regardless of its origin, have a significantly higher adsorption affinity in comparison to PEg, indicating the increase of adsorption affinity with the decrease in MPs' particle size and increase of their specific surface. The results are in accordance with the findings of Wang et al. (2019a).

In comparison between powdered types of MPs, the results (Figs. 1 and 2) also indicate a significantly higher adsorption affinity of PAHs in equilibrium state towards microplastic particles isolated from personal care products (200–320 μg/g) in relation to the PEp

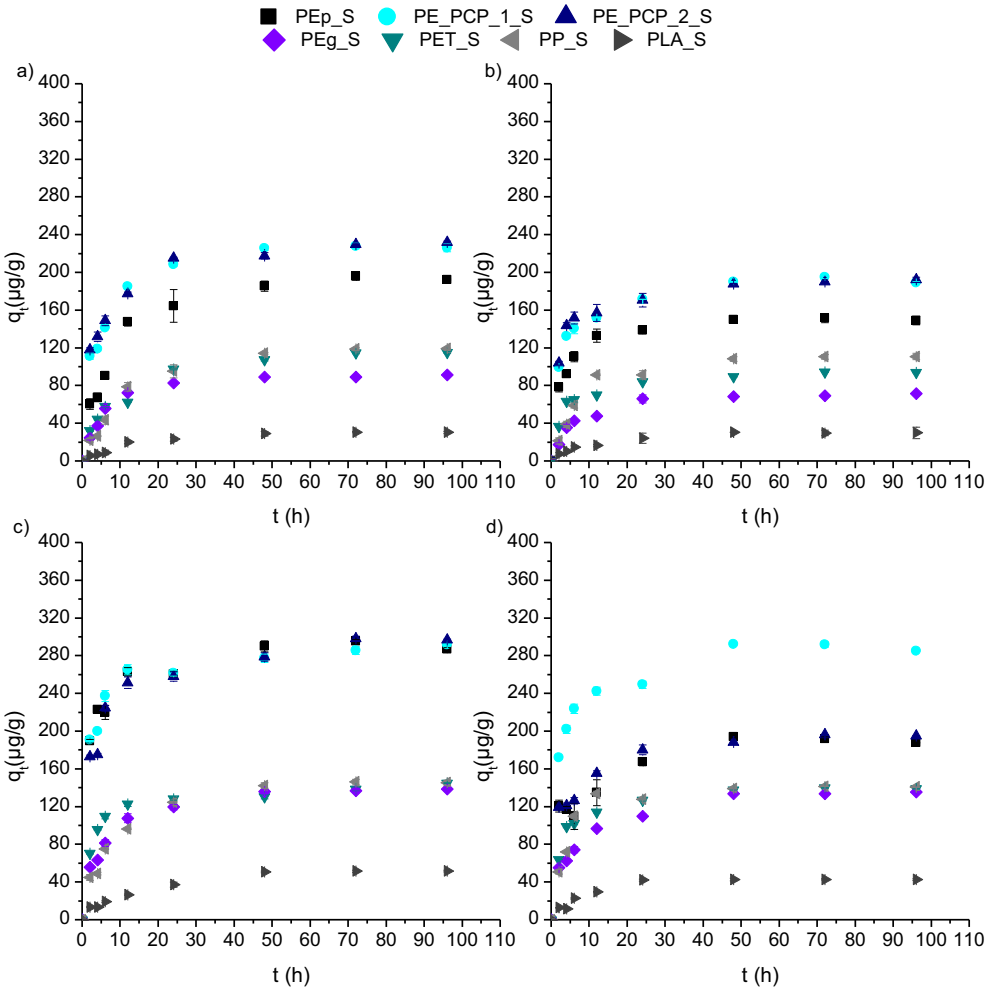

Fig. 1. Kinetic study results (n = 2, mean value ± SD) of: (a) naphthalene, (b) fluorene, (c) fluoranthene and (d) pyrene adsorption on PEp, PE_PCPs_1, PE_PCPs_2, PEg, PET, PP and PLA in the synthetic water matrix.

(140–280 μg/g). The increase of adsorption affinity of MPs isolated from personal care products towards PAHs can be a consequence of the polyethylene structure change, due to the chemical and mechanical treatment of MPs during products' manufacturing process (BET analysis results presented in Table S1). Napper et al. (2015) pointed out the change in the physico-chemical characteristics of microplastics during the industrial production of personal care products. The results are also in accordance with the findings of Wang et al. (2019a), who emphasized that industrial production can cause aging of MPs, resulting in the increase of the adsorption affinity of PAHs to MPs particles.

Furthermore, results presented in Figs. 1 and 2 indicated that the type of microplastic has a significant impact on the adsorption affinity of PAHs. This can be observed by comparing the results achieved for the granulated plastics investigated, which indicated that the degree of PAHs' sorption decreases as follows: PP (115–160 μg/g) > PET (94–144 μg/g) > PEg (75–140 μg/g) > PLA (30–50 μg/g) in both water matrices. By comparing the results of PAHs' adsorption, higher adsorption affinity at equilibrium state was determined for PP than for PET and PEg. Additionally, it can be assumed that functional groups (methyl and terephthalate group) present in the structure of PP and PET respectively are responsible for slightly higher adsorption affinity of selected PAHs, in comparison to PEg and PLA (Fotopoulou and Karapanagioti, 2012; Li et al., 2018b; Torres et al., 2021). Giving the aliphatic structure of PP an intermolecular hydrogen bonding can also occur between selected PAHs and its surface. Furthermore, highly aromatic PET shows stronger adsorption affinity to PAHs due to its hydrophobicity, π–π interactions in comparison to PEg and possible van der Waals interaction. However, molecule size of selected PAHs can reduce the accessibility of active centers and also be responsible for its lower adsorption rate on PET in equilibrium state (F. Wang et al., 2020). Therefore, it can be presumed that a slightly lower adsorption affinity of PAHs to PET in relation to PP occurs due to the difficult PAHs' approach to active centers on the PET surface, which in its structure contains a significantly more voluminous functional group (Balati et al., 2015; Fotopoulou and Karapanagioti, 2012; Fries and Zarfl, 2012; Sørensen et al., 2020). The presence of a methyl group increases the number of available active sites for the formation of bonds between the tested PAHs and PP, which resulted in highest amounts of PAHs adsorbed on this type of granulated microplastic (115–160 μg/g).

In contrast, the lowest adsorption affinity on granulated materials can be observed for PLA, with q_t values for fluoranthene and pyrene in both tested water matrices of about 50 μg/g after 48 h of contact time. Slightly lower affinity for PLA, based on q_t values, was achieved by naphthalene and fluorene (34 μg/g and 30 μg/g, respectively), in both water matrices. The results of PAHs' adsorption on PLA indicate a significantly lower adsorption affinity of these compounds compared to nondegradable MPs, and can be considered as one more advantage of this type of BP. The results are in line with those given by Wang and Wang (2018a) whose study pointed out that adsorption rate of pyrene is impacted by MP type. The oxygen-containing functional groups such as carbonyl group in PLA can also act as H-bond acceptors (Endo et al., 2011; F. Wang et al., 2020). They can interact with water molecules

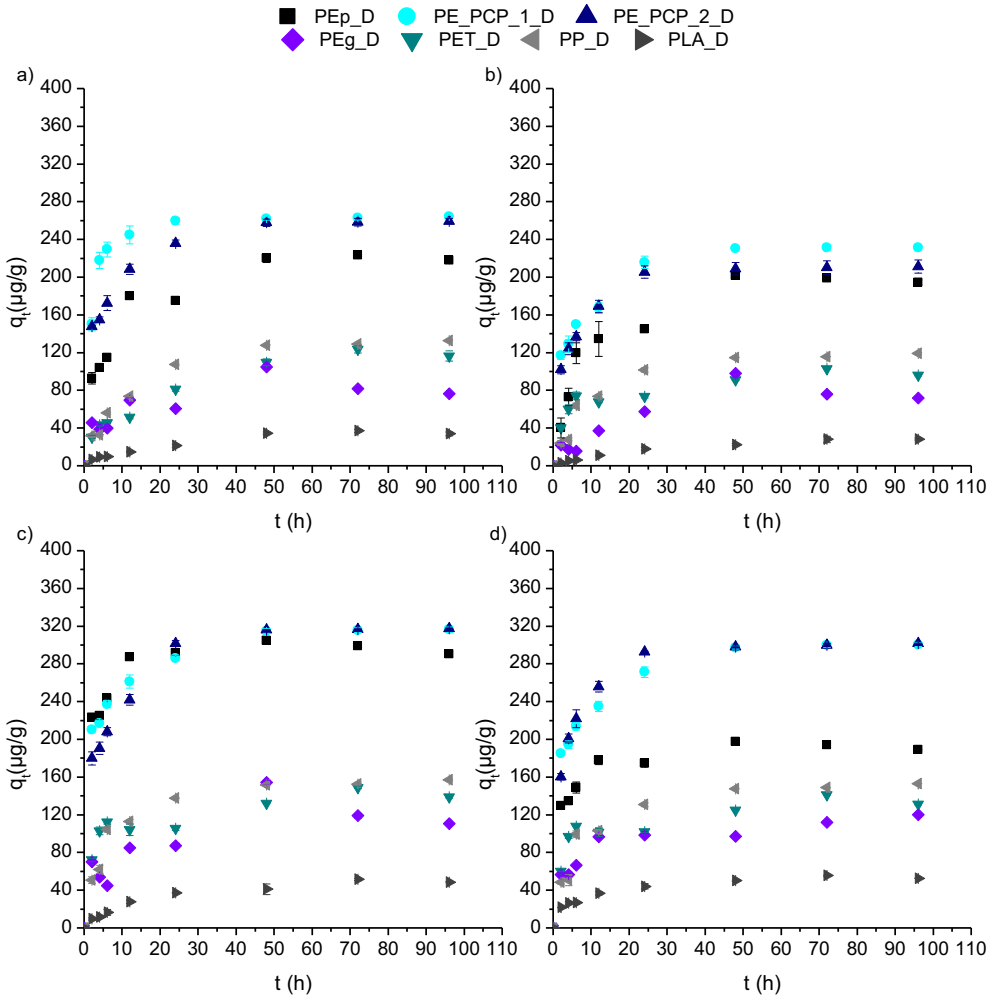

Fig. 2. Kinetic study results (n = 2, mean value ± SD) of: (a) naphthalene, (b) fluorene, (c) fluoranthene and (d) pyrene adsorption on PEp, PE_PCPs_1, PE_PCPs_2, PEg, PET, PP and PLA in the Danube river water.

creating hydrogen bond donors that can form water clusters on the surface of PLA. The formation of three-dimensional water clusters can reduce the accessibility of PAHs and cause lower adsorption rate of selected PAHs on PLA.

In addition to the characteristics of MPs, important factors influencing the adsorption behavior of PAHs are their physico-chemical characteristics, such as water solubility, hydrophobicity and molecular size (Hüffer and Hofmann, 2016; Li et al., 2018a; Wu et al., 2016). The highest adsorption affinity for the selected types of MPs within equilibrium was observed for fluoranthene (q_t = 50–320 µg/g) in both water matrices. A slightly lower affinity was observed for pyrene (q_t = 40–285 µg/g for the synthetic and 50–300 µg/g for real water matrix). The lowest adsorption affinity in terms of q_t values, ranging between 34 and 260 µg/g for synthetic water matrix and 30–230 µg/g for Danube River water, were achieved for adsorption of naphthalene and fluorene towards selected types of MPs after 48 h of contact time. These values are in range of q_t values achieved by Wang and Wang (2018a, 2018b), for similar PAHs' concentration range.

In order to conduct more detailed observation into the adsorption kinetics of PAHs on selected MPs, three widely accepted kinetic models – the pseudo-first- and second-order models, and Weber-Morris (W-M) model – were applied to fit the experimental data (Figs. S3 and S4, Tables 2 and S5). The correlation coefficients (R^2) attained for the pseudo-first order kinetic model were very low (with a maximum of 0.878), suggesting that this kinetic model is not suitable for the interpretation of experimentally attained data; therefore it will not be discussed below. The suitability of pseudo-second order kinetic model for the adsorption process on all MPs was established based on the high values of correlation coefficients (R^2 = 0.916–1.000), presented in Table 2. Satisfactory compliance of adsorption capacity theoretical values compared to experimentally attained values confirmed the validity of the applied pseudo-second order kinetic model for PAHs' adsorption on MPs. The experimentally attained adsorption capacity values (q_e = 165.5–316.5 µg/g) indicated that powdered MPs particles had higher adsorption affinity towards selected PAHs in comparison to granulated types of MPs (q_e = 75.2–153.1 µg/g). The results, given in Table 2, also indicate that PLA particles had the lowest adsorption affinity towards PAHs in both water matrices (q_e = 11.86–55.69 µg/g), in accordance with the maximum adsorbed amounts of this degradable plastic (Figs. 1 and 2). Based on significantly lower values of the pseudo-second order kinetic rate constant (k_2) in relation to the calculated values of the initial sorption rate constant (h) for adsorption of naphthalene, fluorene, fluoranthene and pyrene on the MPs, it can be concluded that the adsorption rate ran significantly faster at the beginning of the adsorption process.

Based on the results for the pseudo-second order kinetic model, it can be assumed that the chemisorption mechanism was responsible for the adsorption of the investigated PAHs on selected types of microplastics. This is in accordance with the results of Wang and Wang (2018a), who indicated that chemisorption was mainly responsible for adsorption of pyrene on three different types of MPs (PE, PS and PVC) in a synthetic water matrix. They pointed out the applicability of the pseudo-second order kinetic model by comparing the

Table 2
Pseudo-second order kinetic model parameters for polycyclic aromatic hydrocarbon adsorption on microplastics.

Compound	MPs	k_2 (g/μg h)	h (g/μg h)	R^2	q_e (theoretical) (μg/g)	q_e (experimental) (μg/g)	SD
Naphthalene	PEp_S	0.0033	120.5	1.000	191.6	192.4	0.59
	PEp_D	0.0052	190.8	1.000	191.6	203.5	8.44
	PE_PCPs_1_S	0.0006	34.88	0.988	238.1	226.3	8.34
	PE_PCPs_1_D	0.0008	54.11	1.000	267.4	264.2	2.23
	PE_PCPs_2_S	0.0017	65.79	1.000	199.6	201.8	1.56
	PE_PCPs_2_D	0.0003	27.84	0.999	307.7	299.6	5.72
	PEg_S	0.0003	255.8	0.996	144.3	135.8	6.01
	PEg_D	0.0014	471.7	0.987	113.1	128.2	10.7
	PET_S	0.0110	64.14	0.967	76.34	75.20	0.80
	PET_D	0.0117	245.1	0.999	144.5	125.1	13.7
	PP_S	0.0036	76.80	0.998	146.8	149.2	1.67
	PP_D	0.0033	84.18	1.000	158.7	153.0	4.09
	PLA_S	0.0975	222.7	0.952	47.80	30.45	12.3
	PLA_D	0.0897	271.7	0.997	55.04	37.24	12.6
Fluorene	PEp_S	0.0050	208.8	0.998	204.5	209.2	3.32
	PEp_D	0.0041	211.0	0.997	227.3	221.8	3.87
	PE_PCPs_1_S	0.0040	145.6	0.996	190.8	195.0	2.95
	PE_PCPs_1_D	0.0037	209.6	0.995	239.2	231.7	5.30
	PE_PCPs_2_S	0.0020	103.4	0.997	227.3	199.3	19.8
	PE_PCPs_2_D	0.0024	163.4	0.993	258.4	231.4	19.1
	PEg_S	0.0145	118.2	0.997	132.6	119.3	9.42
	PEg_D	0.0341	83.82	0.978	117.6	113.9	2.65
	PET_S	0.0110	163.7	0.974	122.1	104.2	12.6
	PET_D	0.0149	214.1	0.982	119.8	103.2	11.7
	PP_S	0.0039	73.91	0.985	138.5	110.9	19.5
	PP_D	0.0017	39.68	0.979	152.2	149.3	2.06
	PLA_S	0.0209	24.83	0.993	34.47	30.14	3.06
	PLA_D	0.0140	24.17	0.915	41.51	48.57	4.99
Fluoranthene	PEp_S	0.0006	14.94	0.999	157.2	165.5	5.85
	PEp_D	0.0002	8.006	0.973	215.1	205.1	7.04
	PE_PCPs_1_S	0.0004	35.71	0.998	293.3	291.7	1.10
	PE_PCPs_1_D	0.0008	81.10	0.997	315.5	316.5	0.74
	PE_PCPs_2_S	0.0005	17.99	1.000	194.6	198.1	2.51
	PE_PCPs_2_D	0.0012	57.54	0.992	216.0	217.6	1.14
	PEg_S	0.0129	17.97	0.998	95.88	91.64	3.00
	PEg_D	0.0127	13.03	0.927	81.23	88.24	4.95
	PET_S	0.0037	32.74	0.997	94.52	105.1	7.50
	PET_D	0.0030	30.62	0.991	101.5	109.0	5.28
	PP_S	0.0049	67.89	0.980	117.6	116.3	0.96
	PP_D	0.0047	75.82	0.993	126.9	137.3	7.35
	PLA_S	0.0326	43.94	0.916	11.72	11.86	0.10
	PLA_D	0.0351	44.66	0.933	35.69	36.72	0.70
Pyrene	PEp_S	0.0001	10.46	0.998	292.4	294.3	1.35
	PEp_D	0.0001	12.10	0.994	292.4	297.5	3.64
	PE_PCPs_1_S	0.0004	32.35	0.999	293.3	292.3	0.68
	PE_PCPs_1_D	0.0002	21.97	0.998	304.0	300.7	2.32
	PE_PCPs_2_S	0.0003	23.06	0.995	300.3	296.5	2.69
	PE_PCPs_2_D	0.0004	41.68	0.999	324.7	301.7	16.2
	PEg_S	0.0033	6.016	0.994	73.96	83.60	6.81
	PEg_D	0.0016	17.94	0.995	90.09	105.9	11.2
	PET_S	0.0002	3.732	0.999	147.5	139.1	5.91
	PET_D	0.0002	3.056	0.995	140.8	141.1	0.18
	PP_S	0.0259	653.6	0.985	158.7	141.7	12.0
	PP_D	0.0001	1.374	0.997	161.3	153.1	5.78
	PLA_S	0.0019	6.078	0.954	56.92	42.96	9.87
	PLA_D	0.0016	4.944	0.988	55.49	55.69	0.14

experimentally attained values of adsorption capacity with the theoretical ones for adsorption of PAHs on MPs.

The plots developed using the W-M intraparticle diffusion model, as applied to the adsorption results of naphthalene, fluorene, fluoranthene and pyrene on selected types of MPs, are shown in Figs. S3 and S4 and Table S5. The results of W-M model are presented as the dependence of the adsorption capacity on $t^{1/2}$. The correlation lines do not pass through the coordinate origin, which implies that intraparticle diffusion was a limiting factor for the adsorption process.

The adsorption of PAHs on PEp is conducted in several phases. In the case of naphthalene, fluorene, fluoranthene and pyrene on PEp in both synthetic and real water matrices adsorption took place mainly in three stages, except in the case of pyrene in synthetic water where two-stage adsorption occurred. The same results were achieved for adsorption of PAHs on PE_PCPs_1 (Figs. S3 and S4). In contrast, the results of W-M kinetic model indicated a two-stage adsorption of PAHs on PE_PCPs_2 in both tested water matrices, except in the case of adsorption of fluorene and fluoranthene on PE_PCPs_2 in a synthetic water matrix, where three stages of adsorption were observed. The W-M kinetic model also fitted attained results for PAHs' adsorption on selected granular types of MPs (PEg, PET, PP and PLA). The results imply that two-stage adsorption took place in both investigated water matrices.

Comparing the results of W-M model for PAHs' adsorption on powdered types of MPs (PEp, PE_PCPs_1 and PE_PCPs_2) and PEg reveals a significant difference in the adsorption steps, indicating that the particle size and origin of MPs had an important role in its adsorption behavior.

In addition, the adsorption of PAHs on PE_PCPs_2 and PEg took place mainly as two-step adsorption in both tested water matrices. In contrast, the adsorption of PAHs on PEp and PE_PCPs_1 occurred mainly through three steps. The difference in the adsorption kinetics of selected PAHs on PEp, PE_PCPs_1 and PE_PCPs_2 may be due to possible changes in the structure of MPs during industrial production (Napper et al., 2015). The fact revealed by W-M model, that powder PE selected from two different personal care products are acting differently, with PE_PCP_1 being similar to PEp and PE_PCP_2 being similar to PEg, confirms that conclusions about MPs' interaction with other pollutants in water cannot be generalized and drawn from the studies only concerning the standard MPs, because the production process obviously changes the structure of the polymers and influences on their behavior in the environment.

In comparing the W-M kinetic model fit for adsorption of naphthalene, fluorene, fluoranthene, and pyrene on granulated MPs (Figs. S3 and S4 and in Table S5), the results indicate a multistage adsorption process. Two-step PAH adsorption is present on PEg, PET and PP and is observed in both water matrices indicating the fast PAHs' adsorption in the form of external diffusion as a first step, while in the second, slower step, an equilibrium state is established. The results also indicated that the first step of naphthalene adsorption on PLA occurs over a significantly longer period in both tested water matrices, probably due to its physico-chemical properties. Namely, as naphthalene has the highest water solubility (Table 1), its tendency towards the solid phase, in this case of PLA, is lower in comparison to the other investigated PAHs. Since the study of PAHs' adsorption was performed in a mixture of selected compounds, the longer duration of external diffusion of naphthalene to the PLA particle could be due to its competition with compounds with lower water solubility, as indicated also by Wang and Wang (2018a).

Based on the presented results of modeling experimental data using the W-M kinetic model, it can be noted that the first two steps of adsorption of selected organic pollutants were controlled by intraparticle diffusion. However, the occurrence of intraparticle diffusion of selected organic pollutants should be taken in account, since the time required for intraparticle diffusion depends on many factors (MPs particle size, temperature, solution concentration, etc.) that are difficult to control in real conditions (Wu et al., 2016; Wang and Wang, 2018a).

3.2. Adsorption isotherms

In order to gain more detailed information about adsorption mechanism of naphthalene, fluorene, fluoranthene and pyrene on selected MPs, the Freundlich, Langmuir, Redlich-Petersen, Tempkin and Dubinine-Radushkevich adsorption models were conducted. Parameters calculated with selected isotherm models for adsorption of PAHs onto MPs particles are summarized in Table S6. The fitted curves for PAHs adsorption on selected MPs using Freundlich and Langmuir adsorption isotherms, as the most commonly used models, are presented in Figs. 3 and 4.

The results of Freundlich adsorption model ($R^2 = 0.707–0.997$) indicate a good exponential fit for the adsorption of naphthalene, fluorene, fluoranthene and pyrene on selected MPs, which was consistent with

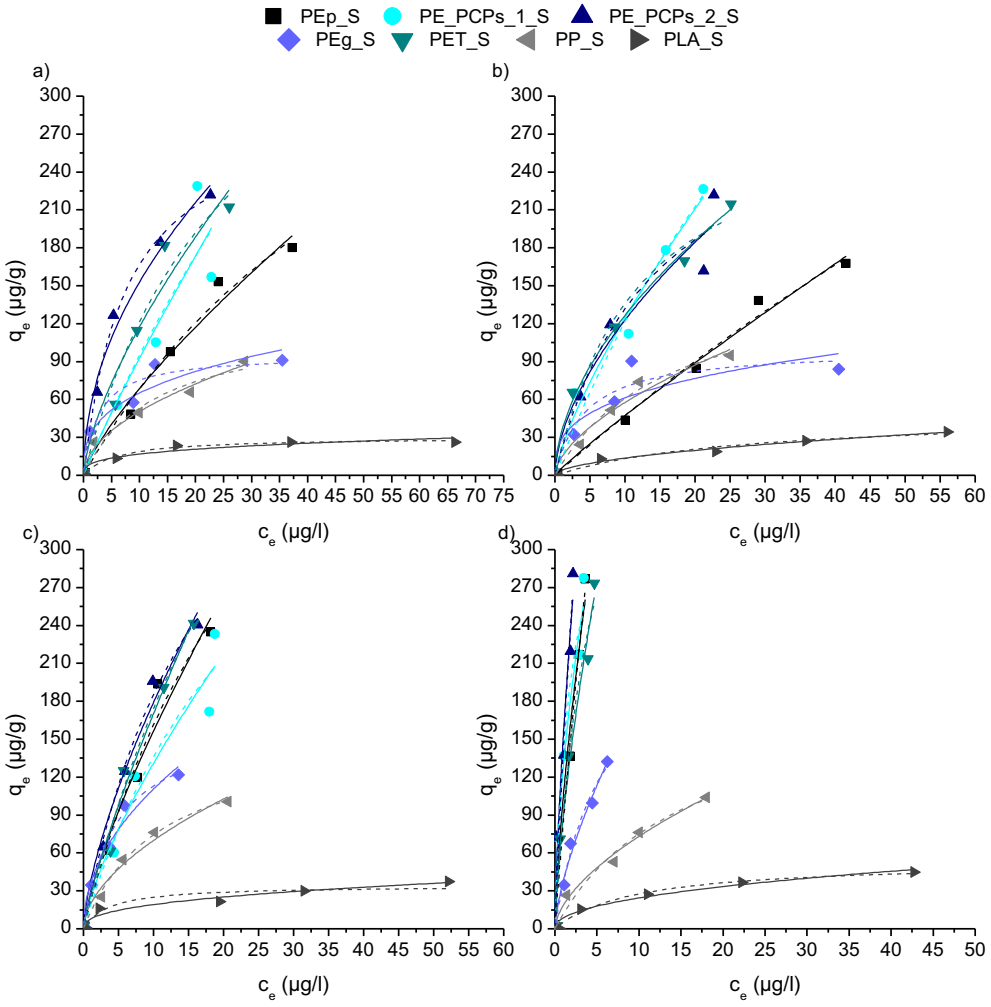

Fig. 3. Adsorption isotherm plots (n = 2, mean value ± SD) for: (a) naphthalene, (b) fluorene, (c) fluoranthene and (d) pyrene on microplastics in synthetic water matrix.

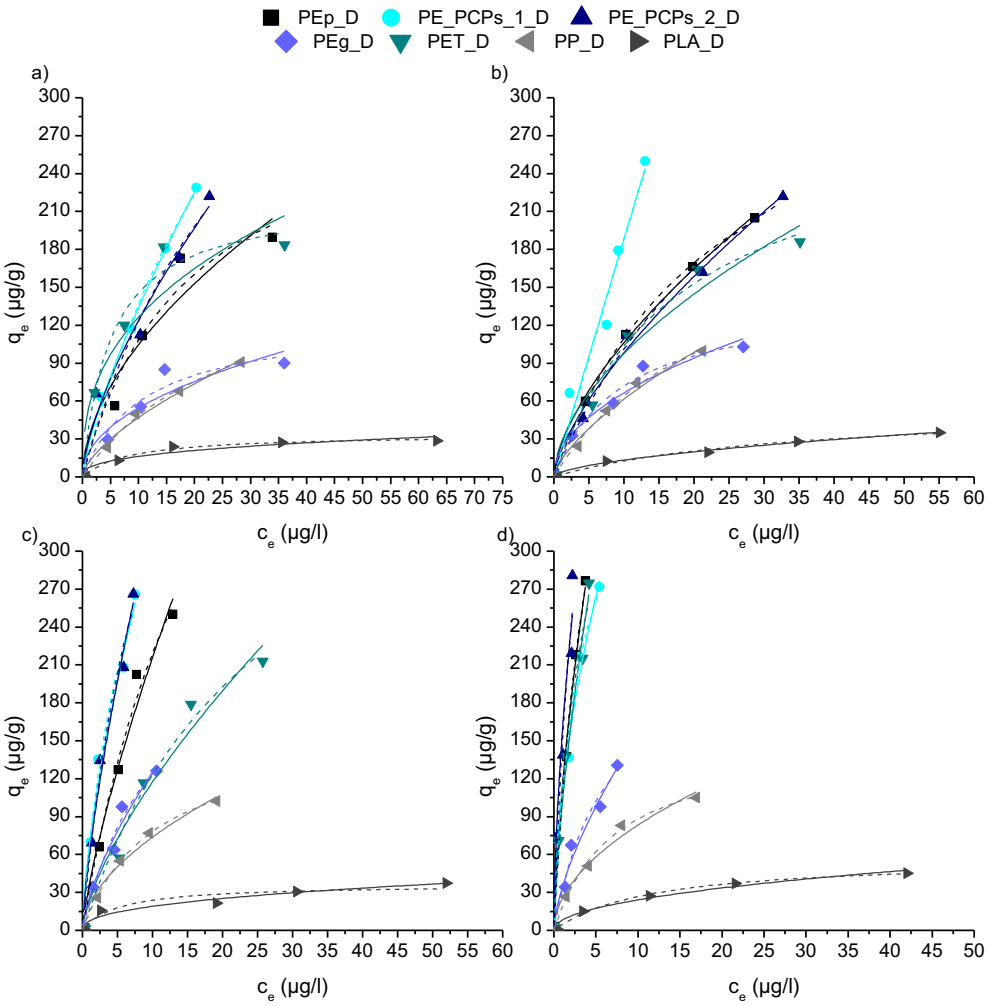

Fig. 4. Adsorption isotherm plots (n = 2, mean value ± SD) for: (a) naphthalene, (b) fluorene, (c) fluoranthene and (d) pyrene on microplastics in real water matrix.

previous studies (Foo and Hameed, 2010; Wang et al., 2019a; Wang and Wang, 2018b). Additionally, recorded values of the Freundlich exponent (n_F = 0.30–0.98) indicated that the adsorption affinity of powdered types of MPs in both investigated water matrices decreased with the increase of initial PAH concentrations. Furthermore, calculated K_F values for Freundlich adsorption model indicated that pyrene had the highest adsorption affinity towards investigated nondegradable MPs (18.6–156.9 (µg/g)/(µg/l)^n). The calculated K_F values were in correlation with studies conducted by Wang et al. (2019b, 2018). They pointed out that K_F values were 3.31–26.3 (µg/g)/(µg/l)^n depending on physico-chemical properties of selected MPs and the investigated organic compound.

In comparison to Freundlich model, the experimental data for PAHs' adsorption onto all selected types of MPs were fitted better by the Langmuir model (R^2 = 0.810–0.999). Langmuir adsorption model parameters indicated significantly high values of maximum adsorption capacity for the adsorption of selected PAHs on powdered types of MPs (q_{max} = 37.34–1676.2 µg/g) in both water matrices. Significantly higher q_{max} values were achieved for the adsorption of naphthalene, fluorene and pyrene on PEp in the synthetic water matrix (504.1 µg/g, 1068.5 µg/g, and 1676.2 µg/g, respectively) compared to Danube River water (308.9 µg/g, 373.6 µg/g, 628.4 µg/g) which indicates a significant influence of water matrix on the adsorption behavior of investigated pollutants. However, water matrix had no significant influence on the adsorption behavior of fluoranthene on PEp, for which the maximum adsorption capacity achieved was 625.0 µg/g and 636.3 µg/g for the synthetic and real water matrix respectively. The influence of water matrix properties was evident within the adsorption of PAHs on PE_PCPs_1 and PE_PCPs_2. The significantly higher maximum adsorption capacities fit for the adsorption of naphthalene, fluorene, fluoranthene and pyrene were achieved in the synthetic water matrix (1024.5 µg/g, 841.2 µg/g, 507.5 µg/g and 1225.4 µg/g, respectively) in relation to Danube River water (619.7 µg/g, 37.34 µg/g, 459.2 µg/g and 619.3 µg/g). An exception occurred during the adsorption of pyrene on PE_PCPs_1, where no significant water impact of adsorption capacity was achieved (382.5 µg/g in synthetic water matrix and 409.7 µg/g in real water matrix).

In this study, the correlation coefficient values for the Langmuir models (R^2 = 0.880–0.985) indicated that the adsorption occurred on the surface of the adsorbent, with a uniform distribution of binding sites and implied formation of monolayer (Zhang et al., 2019, 2020). The impact of water matrix properties was evident in the case of adsorption of naphthalene, fluorene and fluoranthene on PEg, where higher maximum adsorption capacity was calculated for naphthalene, fluorene and fluoranthene in Danube River water, in comparison to synthetic water. In the case of pyrene adsorption on PEg, similar maximum adsorption capacity was achieved in synthetic water matrix (265.2 µg/g), as in Danube water, 253.1 µg/g. A significantly higher maximum adsorption capacity was observed for the PAHs' adsorption on PEp, PE_PCPs_1 and PE_PCPs_2 compared to PEg, probably due to the larger specific surface area for powdered MPs (Guo et al., 2018a; Guo et al., 2018b; Kiso et al., 1999; Luo et al., 2020; Napper et al., 2015).

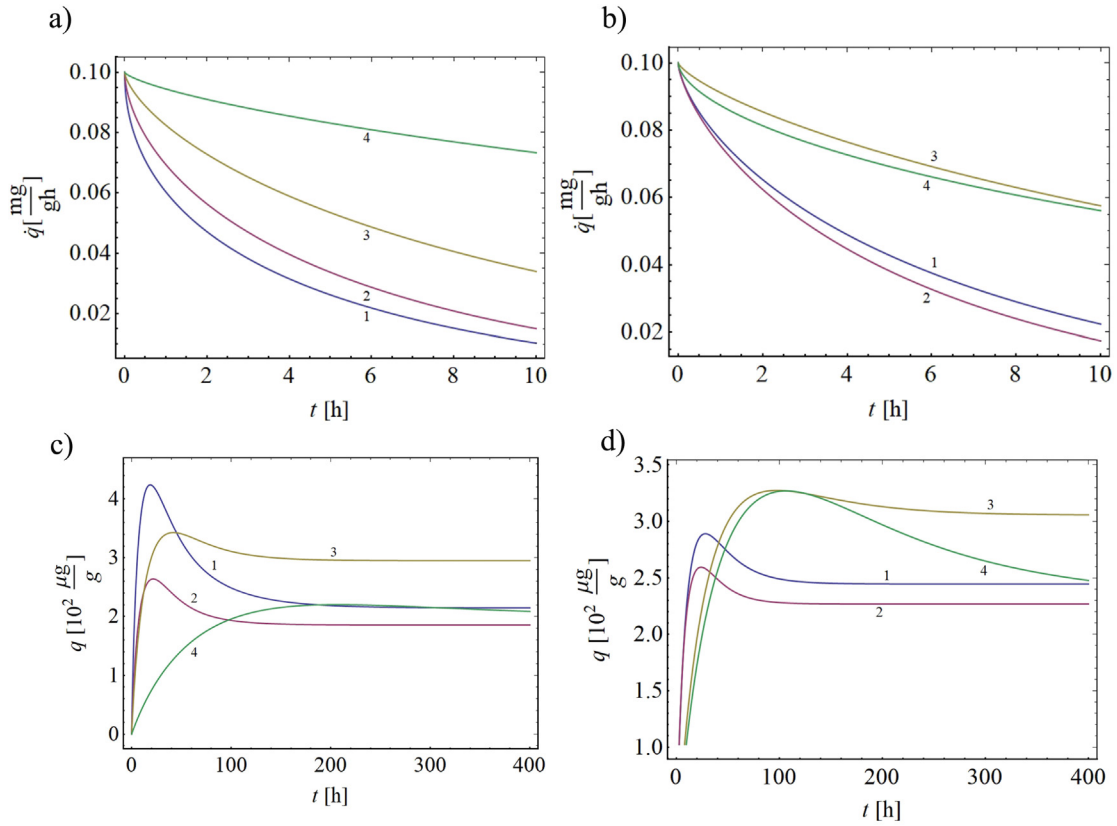

Fig. 5. Sorption rate - time diagrams on: a) PE_PCPs_2_S; b) PE_PCPs_2_D and sorption capacity - time diagrams on: c) PE_PCPs_2_S; d) PE_PCPs_2_D.

Additionally, the high correlation coefficient values of Langmuir model were also achieved for PAHs' adsorption on PET and PP (R^2 = 0.939–0.999). Based on the maximum adsorption capacity values (q_{max}) calculated using Langmuir adsorption model for PAHs adsorption on PET and PP, the influence of water matrix properties was observed. The highest influence of the water matrix properties was indicated for adsorption of pyrene on PET (q_{max} = 2596.5 μg/g) in synthetic water matrix; in comparison, in Danube River water q_{max} was 483.7 μg/g. Significantly lower influence of water characteristics was observed for adsorption of PAHs on PP. As shown in Figs. 3 and 4 and in Table S6, the correlation coefficient of Langmuir isotherm model for adsorption of PAHs on PLA, as a selected representative of BPs, in both water matrices were in a range R^2 = 0.835–0.989. In accordance with the results for nondegradable MPs, the water matrix properties had no significant influence on the maximum adsorption capacity of the PAHs' adsorption on PLA. Additionally, the calculated values of maximum adsorption capacity for PAHs' on PLA in comparison to other selected MPs' particles are up to 10 times lower. Hence, it can be assumed that if PLA, as adsorbent, reaches the environment, the organic pollutant will have significantly lower adsorption affinity towards this type of MP. Therefore, we can suppose that this MP material will not significantly affect the transport of PAHs through the environment.

Redlich-Peterson (R-P), Dubinine-Radushkevich (D-R) and Temkin adsorption isotherm models were also used to get a more detailed investigation of the possible adsorption mechanism. High correlation coefficients were also achieved by applying R-P and D-R models in both water matrices for adsorption of PAHs on all selected types of MPs, R^2 = 0.715–0.999 and R^2 = 0.816–0.999 respectively. The lowest correlation coefficients were achieved for the Temkin model (R^2 = 0.684–0.985). Temkin model indicates that adsorption affinity of PEg decreases with the decrease of available active sites on the MP surface. Due to significantly lower correlation coefficients (Table S6), the Tempkin and R-P models are not the most suitable models in comparison with the other adsorption isotherms applied, which is in accordance with results achieved by Wang and Wang (2018a).

A more detailed insight into the adsorption mechanism of PAHs on selected MPs is achieved by fitting the experimental data with the D-R model. The calculated values of free adsorption energy (E_a) for the adsorption of naphthalene, fluorene and fluoranthene on MPs in the synthetic and real water matrices were in range from 7.50–36.8 kJ/mol. Several authors (Batool et al., 2018; Chen and Chen, 2009; Gupta and Kumar, 2019) studying the modeling of thermodynamic adsorption isotherms for various organic and inorganic pollutants had indicated that the achieved values of adsorption energy (>8 kJ/mol) implied a chemisorption mechanism. Taking those studies into account, the results confirmed that the chemisorption mechanism is responsible for the adsorption of naphthalene, fluorene, fluoranthene and pyrene on selected types of MPs in both water matrices (Chen and Chen, 2009; Dada et al., 2012; Das et al., 2014; Gupta and Kumar, 2019; Wang and Wang, 2018b).

3.3. Mathematical modeling for further interaction mechanism understanding

Guo and Wang (2019) investigated the effect of external and internal adsorption by following the Freundlich adsorption isotherm. They concluded that the external mass transfer was almost equal to the overall adsorption rate, while the influence of the internal mass transfer was negligible.

Based on the adsorption results (Table S6) and BET results (Table S1), the highest adsorption capacity was established for PE_PCPs_2_S and PE_PCPs_2_D. PE_PCPs_2 features enhanced adsorptive affinity for PAHs, due to the largest BET surface area (5.791 m^2/g) and meso-pore

volume (0.099 cm^3/g) in comparison to other MPs, implying to higher uptake of PAHs by PE_PCPs_2. In that way, mathematical model can predict that mass transfer will be occurred on the porous surface. Therefore, the kinetics data of PAHs sorption onto PE_PCPs_2_S and PE_PCPs_2_D were fitted according to the proposed modified model. Using the results of the isotherm experiment, coefficients necessary for mathematical calculation are obtained.

Using relations (11) and (12), variation of the adsorption capacity and adsorption rate in time for naphthalene, fluorene, fluoranthene and pyrene on PE_PCPs_2_S and PE_PCPs_2_D is analyzed. In Fig. 5(a–d) the sorption rate - time and the sorption capacity - time for naphthalene (1), fluorene (2), fluoranthene (3) and pyrene (4) onto PE_PCPs_2_S and PE_PCPs_2_D are plotted, respectively. In Fig. 5c and d the experimentally obtained values plotted in Figs. 1 and 2 are also shown. It gives us the possibility to compare the experimental and mathematical values.

Analyzing the diagrams, it is found that the adsorption rates for all of PAHs is decreasing in time and tends to zero, while the sorption capacity is increasing up to a limit value, which is in accordance with the pseudo-second order kinetic data. The changes of the sorption rate and adsorption capacity have different trend for PAHs. The change of both values is the slowest for pyrene and the fastest for naphthalene. In terms of both MPs, the largest values were achieved for pyrene which is in correlation with highest K_F value for selected PAHs. The uptake of naphthalene, fluorene and fluoranthene by PE_PCPs_2_S and PE_PCPs_2_D increased rapidly within the first hour, and then the sorption rate slowed down with time until equilibrium. Different sorption behavior was observed for pyrene. There was a difference for adsorption capacity over time for fluorene on PE_PCPs_2_S and PE_PCPs_2_D. The difference was reflected in a significantly higher adsorption capacity determined for its adsorption on PE_PCPs_2_S in comparison to PE_PCPs_2_D.

The adsorption capacity time distribution for naphthalene and fluorene was almost the same in the both investigated water matrices. The adsorption capacity for these two PAHs on polyethylene isolated from personal care products was much smaller than for pyrene. Based on the results presented in Fig. 5, the adsorption capacity of PAHs on PE_PCPs_2_D was almost two times smaller than the adsorption capacity calculated for PE_PCPs_2_S but for the both cases the constant value was reached in a short time. Established pseudo-second order and W-M kinetic model results were in correlation with mathematical modeling, which implies to the conduction of external mass transfer of PAHs onto PE_PCPs_2.

Comparing the curves in Fig. 5(a–d) it is obvious that the difference between results computed analytically, by applying the suggested mathematical model, and those obtained experimentally for the real systems (Figs. 1 and 2), is negligible. The limit values for the sorption capacity obtained experimentally and mathematically for naphthalene, fluorene, fluoranthene and pyrene on PE_PCPs_2_S are 240 μg/g and 237 μg/g, 210 μg/g and 203 μg/g, 320 μg/g and 312, 195 μg/g and 190 μg/g, respectively, and on PE_PCPs_2_D are 255 μg/g and 236 μg/g, 225 μg/g and 204 μg/g, 315 μg/g and 304, 290 μg/g and 270 μg/g. It proves that the model proposed in the paper is convenient for solving adsorption problems in PAHs with MPs.

The application of the model is expected to give good results in prediction of adsorption capacity - time relations for other types of PAHs in future, too. The advantage of the model is also reflected in the ability to gives the analytic description of the adsorption rate - time relation, which is important in explanation of PAHs adsorbing with MPs. The time considered in computation of the adsorption capacity - time diagram was longer than that used in experiment (Figs. 1 and 2). Intention was to predict the adsorption tendency in time. It was seen that after certain time the adsorption capacity tends to a constant value (Fig. 5).

4. Conclusion

In this study kinetic adsorption modeling, as well as a mass transfer mathematical model, were applied for better understanding of PAHs' adsorption behavior on nondegradable and degradable microplastics. The results indicated that PAHs showed different adsorption affinities towards the tested microplastic particles. Mathematical modeling confirmed external mass transfer of PAHs onto MP particles, chemisorption mechanism, and pyrene as having the highest adsorption capacity.

The adsorption affinity of PAHs is the most affected by the physico-chemical properties of MPs, such as structure, pore size, specific surface area and granulation. MPs isolated from cosmetic care products showed the highest capacities to adsorb investigated PAHs, indicating that further studies need to be conducted on already used and aged MPs in order to give estimations relevant for real environment conditions. Granulated MPs have lower affinity for PAHs' adsorption, with PP showing the highest and PLA the lowest affinity in this group. These results indicate that PLA, as representative of BPs, could have significantly less impact on PAHs' transport through the environment. Physico-chemical properties of selected PAHs have also impacted on adsorption affinity, as well as the water matrix. However, these two factors are less pronounced compared to the influence of MP type.

CRediT authorship contribution statement

Maja Lončarski: conceptualization, visualization, methodology, investigation, writing-original draft preparation, writing–review and editing, chemical analysis. **Vesna Gvoić:** data analysis, writing-review and editing; **Livija Cveticanin:** development of new mathematical model. **Aleksandra Tubić:** conceptualization of this study, writing–review and editing. **Miljana Prica:** Writing-review and editing. **Miljana Prica** and **Jasmina Agbaba:** resources and funding acquisition. All authors read and approved the final manuscript.

Declaration of competing interest

The authors declare that they have no known competing financial interests or personal relationships that could have appeared to influence the work reported in this paper.

Acknowledgments

The authors acknowledge financial support of the Ministry of Education, Science and Technological Development of the Republic of Serbia (Grant No. 451-03-9/2021-14/200125 and Grant No. 451-03-9/2021-14/200156).

Novelty statement

The novelty and scientific significance of the research article is stated through the investigated and clarified adsorption behavior of polycyclic aromatic hydrocarbons on microplastic particles, bringing attention to both polycyclic aromatic hydrocarbons and microplastics which have not been extensively studied so far, especially biodegradable plastic materials. The additional knowledge about polycyclic aromatic hydrocarbons adsorption mechanism on microplastics in freshwater is emphasized. The usage of various sorption kinetics and isotherm models, followed by mass transfer mathematical model, contributed to better understanding of interactions occurred between polycyclic aromatic hydrocarbons and microplastics, as well as pollution adsorption behavior on non-degradable and degradable microplastics.

Appendix A. Supplementary data

Supplementary data to this article can be found online at https://doi.org/10.1016/j.scitotenv.2021.147289.

References

APHA, 1982. Standard Methods for the Examination of Water and Wastewater. 16. Am. Public Heal. Assoc. Am. Water Work. Assoc. Water Environ. Fed., pp. 1495–1497.

Avio, G.C., Gorbi, S., Milan, M., Benedetti, M., Fattorini, D., D'Errico, G., Pauletto, M., Bargelloni, L., Regoli, F., 2015. Pollutants bioavailability and toxicological risk from microplastics to marine mussels. Environ. Pollut. 198, 211–222. https://doi.org/10.1016/j.envpol.2014.12.021.

Bakir, A., Rowland, S.J., Thompson, R.C., 2014. Enhanced desorption of persistent organic pollutants from microplastics under simulated physiological conditions. Environ. Pollut. 185, 16–23. https://doi.org/10.1016/j.envpol.2013.10.007.

Balati, A., Shahbazi, A., Amini, M.M., Hashemi, S.H., 2015. Adsorption of polycyclic aromatic hydrocarbons from wastewater by using silica-based organic–inorganic nanohybrid material. J. Water Reuse Desal. 5, 50–63. https://doi.org/10.2166/wrd.2014.013.

Batool, F., Akbar, J., Iqbal, S., Noreen, S., Bukhari, S.N., 2018. Study of isothermal, kinetic, and thermodynamic parameters for adsorption of cadmium: an overview of linear and nonlinear approach and error analysis. Bioinorg. Chem. Appl. 2018. https://doi.org/10.1155/2018/3463724.

Chae, Y., An, Y.-J.J., 2017. Effects of micro- and nanoplastics on aquatic ecosystems: current research trends and perspectives. Mar. Pollut. Bull. 124, 624–632. https://doi.org/10.1016/j.marpolbul.2017.01.070.

Chen, A.H., Chen, S.M., 2009. Biosorption of azo dyes from aqueous solution by glutaraldehyde-crosslinked chitosans. J. Hazard. Mater. 172, 1111–1121. https://doi.org/10.1016/j.jhazmat.2009.07.104.

Cveticanin, L., 2012. A review on dynamics of mass variable systems. J.Serb. Soc. Comput. Mech. 6, 56–73.

Cveticanin, L., 2014. Dynamics of the mass variable body. In: Irschik, H., Belyaev, A.K. (Eds.), Dynamics of Mechanical Systems With Variable Mass. CISM International Centre for Mechanical Sciences. vol. 557. Springer, Vienna, pp. 107–164.

Cveticanin, L., 2016. Dynamics of Bodies With Time-variable Mass. Springer, Vienna.

Dada, A., Olalekan, A., Olatunya, A., O, Dada, 2012. Langmuir, Freundlich, Temkin and Dubinin–Radushkevich isotherms studies of equilibrium sorption of Zn 2+ unto phosphoric acid modified rice husk. IOSR J. Appl. Chem. 3, 38–45. https://doi.org/10.9790/5736-0313845.

Das, B., Mondal, N.K., Bhaumik, R., Roy, P., 2014. Insight into adsorption equilibrium, kinetics and thermodynamics of lead onto alluvial soil. Int. J. Environ. Sci. Technol. 11, 1101–1114. https://doi.org/10.1007/s13762-013-0279-z.

Devriese, L.I., Witte, B. De, Vethaak, A.D., Hostens, K., Leslie, H.A., 2017. Chemosphere bioaccumulation of PCBs from microplastics in Norway lobster (Nephrops norvegicus): an experimental study. Chemosphere 186, 10–16. https://doi.org/10.1016/j.chemosphere.2017.07.121.

Directive, 2013. Directives of 12 August 2013 amending Directives 2000/60/EC and 2008/105/EC as regards priority substances in the field of water policy. Off. J. Eur. Union 2013, 1–17. http://eur-lex.europa.eu/legal-content/EN/TXT/?uri=celex:32013L0039.

Directive 2000/60/EC, 2000. Directive 2000/60/EC of the European Parliament and of the council of 23 October 2000 establishing a framework for community action in the field of water policy. Off. J. Eur. Communities L 327, 1–73.

Endo, S., Droge, S.T.J., Goss, K.-U., 2011. Polyparameter linear free energy models for polyacrylate. Anal. Chem. 83, 1394–1400.

Fan, X., Zou, Y., Geng, N., Liu, J., Hou, J., Li, D., Yang, C., Li, Y., 2021. Investigation on the adsorption and desorption behaviors of antibiotics by degradable MPs with or without UV ageing process. J. Hazard. Mater. 401, 123363. https://doi.org/10.1016/j.jhazmat.2020.123363.

Farrell, P., Nelson, K., 2013. Trophic level transfer of microplastic: Mytilus edulis (L.) to Carcinus maenas (L.). Environ. Pollut. 177, 1–3. https://doi.org/10.1016/j.envpol.2013.01.046.

Foo, K.Y., Hameed, B.H., 2010. Insights into the modeling of adsorption isotherm systems. Chem. Eng. J. 156, 2–10. https://doi.org/10.1016/j.cej.2009.09.013.

Fotopoulou, K.N., Karapanagioti, H.K., 2012. Surface properties of beached plastic pellets. Mar. Environ. Res. 81, 70–77. https://doi.org/10.1016/j.marenvres.2012.08.010.

Frias, J.P.G.L., Sobral, P., Ferreira, A.M., 2010. Organic pollutants in microplastics from two beaches of the Portuguese coast. Mar. Pollut. Bull. 60, 1988–1992. https://doi.org/10.1016/j.marpolbul.2010.07.030.

Fries, E., Zarfl, C., 2012. Sorption of polycyclic aromatic hydrocarbons (PAHs) to low and high density polyethylene (PE). Environ. Sci. Pollut. Res. 19, 1296–1304. https://doi.org/10.1007/s11356-011-0655-5.

Green, D.S., Boots, B., Sigwart, J., Jiang, S., Rocha, C., 2016. Effects of conventional and biodegradable microplastics on a marine ecosystem engineer (Arenicola marina) and sediment nutrient cycling. Environ. Pollut. 208, 426–434. https://doi.org/10.1016/j.envpol.2015.10.010.

Guo, W., Wang, S., Wang, Y., Lu, S., Gao, Y., 2018b. Sorptive removal of phenanthrene from aqueous solutions using magnetic and non-magnetic rice husk-derived biochars. R. Soc. Open Sci. 5. https://doi.org/10.1098/rsos.172382.

Guo, X., Wang, J., 2019. The phenomenological mass transfer kinetics model for Sr2+ sorption onto spheroids primary microplastics. Environ. Pollut. 250, 737–745. https://doi.org/10.1016/j.envpol.2019.04.091.

Guo, X., Pang, J., Chen, S., Jia, H., 2018a. Sorption properties of tylosin on four different microplastics. Chemosphere 209, 240–245. https://doi.org/10.1016/j.chemosphere.2018.06.100.

Gupta, S., Kumar, A., 2019. Removal of nickel (II) from aqueous solution by biosorption on A. barbadensis Miller waste leaves powder. Appl Water Sci 9, 1–11. https://doi.org/10.1007/s13201-019-0973-1.

Hahladakis, J.N., Velis, C.A., Weber, R., Iacovidou, E., Purnell, P., 2018. An overview of chemical additives present in plastics: migration, release, fate and environmental impact during their use, disposal and recycling. J. Hazard. Mater. 344, 179–199. https://doi.org/10.1016/j.jhazmat.2017.10.014.

Hüffer, T., Hofmann, T., 2016. Sorption of non-polar organic compounds by micro-sized plastic particles in aqueous solution. Environ. Pollut. 214, 194–201. https://doi.org/10.1016/j.envpol.2016.04.018.

Kiso, Y., Kitao, T., Nishimura, K., 1999. Adsorption properties of aromatic compounds on polyethylene as a membrane material. J. Appl. Polym. Sci. 74, 1037–1043. https://doi.org/10.1002/(SICI)1097-4628(19991031)74:5<1037::AID-APP1>3.0.CO;2-L.

Koelmans, A.A., Bakir, A., Burton, G.A., Janssen, C.R., 2016. Microplastic as a vector for chemicals in the aquatic environment: critical review and model-supported reinterpretation of empirical studies. Environ. Sci. Technol. 50, 3315–3326. https://doi.org/10.1021/acs.est.5b06069.

Koelmans, A.A., Mohamed Nor, N.H., Hermsen, E., Kooi, M., Mintenig, S.M., De France, J., 2019. Microplastics in freshwaters and drinking water: critical review and assessment of data quality. Water Res. 155, 410–422. https://doi.org/10.1016/j.watres.2019.02.054.

Kyoung Song, Y., Hee Hong, S., Jang, M., Myung Han, G., Won Jung, S., Joon Shim, W., 2017. Combined Effects of UV Exposure Duration and Mechanical Abrasion on Microplastic Fragmentation by Polymer Type. https://doi.org/10.1021/acs.est.6b06155.

Li, Jia, Zhang, K., Zhang, H., 2018b. Adsorption of antibiotics on microplastics. Environ. Pollut. 237, 460–467. https://doi.org/10.1016/j.envpol.2018.02.050.

Li, Jingyi, Liu, H., Paul Chen, J., 2018a. Microplastics in freshwater systems: a review on occurrence, environmental effects, and methods for microplastics detection. Water Res. 137, 362–374. https://doi.org/10.1016/J.WATRES.2017.12.056.

Liu, L., Fokkink, R., Koelmans, A.A., 2016. Sorption of polycyclic aromatic hydrocarbons to polystyrene nanoplastic. Environ. Toxicol. Chem. 35, 1650–1655. https://doi.org/10.1002/etc.3311.

Lončarski, M., Tubić, A., Isakovski, Kragulj, Marijana Jović, B., Apostolović, T., Nikić, J., Agbaba, J., 2020. Modeling of the adsorption of chlorinated phenols adsorption on polyethylene and polyethylene terephtalate microplastic. J. Serb. Chem. Soc. 85 (5), 697–709. https://doi.org/10.2298/JSC190712124L.

Luo, H., Zhao, Y., Li, Y., Xiang, Y., He, D., Pan, X., 2020. Aging of microplastics affects their surface properties, thermal decomposition, additives leaching and interactions in simulated fluids. Sci. Total Environ. 714, 136862. https://doi.org/10.1016/J.SCITOTENV.2020.136862.

Mojiri, A., Zhou, J.L., Ohashi, A., Ozaki, N., Kindaichi, T., 2019. Comprehensive review of polycyclic aromatic hydrocarbons in water sources, their effects and treatments. Sci. Total Environ. 696, 133971. https://doi.org/10.1016/j.scitotenv.2019.133971.

Napper, I.E., Bakir, A., Rowland, S.J., Thompson, R.C., 2015. Characterisation, quantity and sorptive properties of microplastics extracted from cosmetics. Mar. Pollut. Bull. 99, 178–185. https://doi.org/10.1016/j.marpolbul.2015.07.029.

Niederer, C., Schwarzenbach, R.P., Goss, K.U., 2007. Elucidating differences in the sorption properties of 10 humic and fulvic acids for polar and nonpolar organic chemicals. Environ. Sci. Technol. 41, 6711–6717. https://doi.org/10.1021/es0709932.

Nuelle, M.T., Dekiff, J.H., Remy, D., Fries, E., 2014. A new analytical approach for monitoring microplastics in marine sediments. Environ. Pollut. 184, 161–169. https://doi.org/10.1016/j.envpol.2013.07.027.

Oliveira, M., Ribeiro, A., Hylland, K., Guilhermino, L., 2013. Single and combined effects of microplastics and pyrene on juveniles (0+ group) of the common goby Pomatoschistus microps (Teleostei, Gobiidae). Ecol. Indic. 34, 641–647. https://doi.org/10.1016/j.ecolind.2013.06.019.

Patel, A.B., Shaikh, S., Jain, K.R., Desai, C., 2020. Polycyclic Aromatic Hydrocarbons: Sources, Toxicity, and Remediation Approaches. 11. https://doi.org/10.3389/fmicb.2020.562813.

Prunier, J., Maurice, L., Perez, E., Gigault, J., Pierson Wickmann, A.C., Davranche, M., Halle, A. ter, 2019. Trace metals in polyethylene debris from the North Atlantic subtropical gyre. Environ. Pollut. 245, 371–379. https://doi.org/10.1016/j.envpol.2018.10.043.

Rios Mendoza, L.M., Balcer, M., 2020. Microplastics in Freshwater Environments, Encyclopedia of the World's Biomes. Elsevier Inc https://doi.org/10.1016/b978-0-12-409548-9.12394-2.

Rochman, C.M., Manzano, C., Hentschel, B.T., Simonich, S.L.M., Hoh, E., 2013. Polystyrene plastic: a source and sink for polycyclic aromatic hydrocarbons in the marine environment. Environ. Sci. Technol. 47, 13976–13984. https://doi.org/10.1021/es403605f.

Rodrigues, J.P., Duarte, A.C., Santos-Echeandía, J., Rocha-Santos, T., 2019. Significance of interactions between microplastics and POPs in the marine environment: a critical overview. TrAC Trends Anal. Chem. 111, 252–260. https://doi.org/10.1016/j.trac.2018.11.038.

Scopetani, C., Cincinelli, A., Martellini, T., Lombardini, E., Ciofini, A., Fortunati, A., Pasquali, V., Ciattini, S., Ugolini, A., 2018. Ingested microplastic as a two-way transporter for PBDEs in Talitrus saltator. Environ. Res. 167, 411–417. https://doi.org/10.1016/j.envres.2018.07.030.

Sjollema, S.B., Redondo-Hasselerharm, P., Leslie, H.A., Kraak, M.H.S., Vethaak, A.D., 2016. Do plastic particles affect microalgal photosynthesis and growth? Aquat. Toxicol. 170, 259–261. https://doi.org/10.1016/j.aquatox.2015.12.002.

Sørensen, L., Rogers, E., Altin, D., Salaberria, I., Booth, A.M., 2020. Sorption of PAHs to microplastic and their bioavailability and toxicity to marine copepods under co-exposure conditions. Environ. Pollut. 258, 113844. https://doi.org/10.1016/j.envpol.2019.113844.

Tan, X., Yu, X., Cai, L., Wang, J., Peng, J., 2019. Microplastics and associated PAHs in surface water from the Feilaixia Reservoir in the Beijiang River, China. Chemosphere 221, 834–840. https://doi.org/10.1016/j.chemosphere.2019.01.022.

Teuten, E.L., Rowland, S.J., Galloway, Tamara Susan, Galloway, Tamara S., 2016. Potential for plastics to transport hydrophobic contaminants potential for plastics to transport hydrophobic contaminants. ACS Publ. 41, 7759–7764. https://doi.org/10.1021/es071737s.

Thompson, R.C., Olson, Y., Mitchell, R.P., Davis, A., Rowland, S.J., John, A.W.G., McGonigle, D., Russell, A.E., 2004. Lost at sea: where is all the plastic? Science 80-.). 304, 838. https://doi.org/10.1126/science.1094559.

Thushari, G.G.N., Senevirathna, J.D.M., Yakupitiyage, A., Chavanich, S., 2017. Effects of microplastics on sessile invertebrates in the eastern coast of Thailand: an approach to coastal zone conservation. Mar. Pollut. Bull. 124, 349–355. https://doi.org/10.1016/j.marpolbul.2017.06.010.

Torres, F.G., Dioses-Salinas, D.C., Pizarro-Ortega, C.I., De-la-Torre, G.E., 2021. Sorption of chemical contaminants on degradable and non-degradable microplastics: recent progress and research trends. Sci. Total Environ. https://doi.org/10.1016/j.scitotenv.2020.143875.

Tubić, A., Lončarski, M., Maletić, S., Molnar Jazić, J., Watson, M., Tričković, J., Agbaba, J., Jazić, J.M., Watson, M., Tričković, J., Agbaba, J., 2019. Significance of chlorinated phenols adsorption on plastics and bioplastics during water treatment. 11, 2358. https://doi.org/10.3390/w11112358.

Tubić, A., Lončarski, M., Apostolović, T., Kragulj Isakovski, M., Tričković, J., Molnar Jazić, J., Agbaba, J., 2021. Adsorption mechanisms of chlorobenzenes and trifluralin on primary polyethylene microplastics in the aquatic environment. Environ. Sci. Pollut. Res. https://doi.org/10.1007/s11356-020-11875-w.

US EPA, 2014. Priority pollutant list. Effl. Guidel. 2.

Wang, C., Zhao, J., Xing, B., 2020a. Environmental source, fate, and toxicity of microplastics. J. Hazard. Mater. https://doi.org/10.1016/j.jhazmat.2020.124357.

Wang, F., Gao, J., Zhai, W., Liu, D., Zhou, Z., Wang, P., 2020c. The influence of polyethylene microplastics on pesticide residue and degradation in the aquatic environment. J. Hazard. Mater. 394, 122517. https://doi.org/10.1016/j.jhazmat.2020.122517.

Wang, F., Zhang, M., Sha, W., Wang, Y., Hao, H., Dou, Y., Li, Y., 2020d. Sorption behavior and mechanisms of organic contaminants to nano and microplastics. Molecules https://doi.org/10.3390/molecules25081827.

Wang, J., Liu, X., Liu, G., 2019a. Sorption behaviors of phenanthrene, nitrobenzene, and naphthalene on mesoplastics and microplastics. Environ. Sci. Pollut. Res. 26, 12563–12573. https://doi.org/10.1007/s11356-019-04735-9.

Wang, J., Liu, X., Liu, G., Zhang, Z., Wu, H., Cui, B., Bai, J., Zhang, W., 2019b. Size effect of polystyrene microplastics on sorption of phenanthrene and nitrobenzene. Ecotoxicol. Environ. Saf. 173, 331–338. https://doi.org/10.1016/j.ecoenv.2019.02.037.

Wang, T., Wang, L., Chen, Q., Kalogerakis, N., Ji, R., Ma, Y., 2020b. Interactions between microplastics and organic pollutants: effects on toxicity, bioaccumulation, degradation, and transport. Sci. Total Environ. https://doi.org/10.1016/j.scitotenv.2020.142427.

Wang, W., Wang, J., 2018a. Different partition of polycyclic aromatic hydrocarbon on environmental particulates in freshwater: microplastics in comparison to natural sediment. Ecotoxicol. Environ. Saf. 147, 648–655. https://doi.org/10.1016/j.ecoenv.2017.09.029.

Wang, W., Wang, J., 2018b. Comparative evaluation of sorption kinetics and isotherms of pyrene onto microplastics. Chemosphere 193, 567–573. https://doi.org/10.1016/j.chemosphere.2017.11.078.

Wang, Z., Chen, M., Zhang, L., Wang, K., Yu, X., Zheng, Z., Zheng, R., 2018. Sorption behaviors of phenanthrene on the microplastics identified in a mariculture farm in Xiangshan Bay, southeastern China. Sci. Total Environ. 628–629, 1617–1626. https://doi.org/10.1016/J.SCITOTENV.2018.02.146.

Wardrop, P., Shimeta, J., Nugegoda, D., Morrison, P.D., Miranda, A., Tang, M., Clarke, B.O., 2016. Chemical pollutants sorbed to ingested microbeads from personal care products accumulate in fish. Environ. Sci. Technol. 50, 4037–4044. https://doi.org/10.1021/acs.est.5b06280.

Weinstein, J.E., Dekle, J.L., Leads, R.R., Hunter, R.A., 2020. Degradation of bio-based and biodegradable plastics in a salt marsh habitat: another potential source of microplastics in coastal waters. Mar. Pollut. Bull. 160, 111518. https://doi.org/10.1016/j.marpolbul.2020.111518.

Wu, C., Zhang, K., Huang, X., Liu, J., 2016. Sorption of pharmaceuticals and personal care products to polyethylene debris. Environ. Sci. Pollut. Res. 23, 8819–8826. https://doi.org/10.1007/s11356-016-6121-7.

Yang, L., Zhang, Y., Kang, S., Wang, Z., Wu, C., 2021. Microplastics in freshwater sediment: a review on methods, occurrence, and sources. Sci. Total Environ. https://doi.org/10.1016/j.scitotenv.2020.141948.

Yu, Z., Lin, Q., Gu, Y., Du, F., Wang, X., Shi, F., Ke, C., Xiang, M., Yu, Y., 2019. Ecotoxicology and environmental safety bioaccumulation of polycyclic aromatic hydrocarbons (PAHs) in wild marine fi sh from the coastal waters of the northern South China Sea: risk assessment for human health. Ecotoxicol. Environ. Saf. 180, 742–748. https://doi.org/10.1016/j.ecoenv.2019.05.065.

Zhang, C., Chen, X., Wang, J., Tan, L., 2017. Toxic effects of microplastic on marine microalgae Skeletonema costatum: interactions between microplastic and algae. Environ. Pollut. 220, 1282–1288. https://doi.org/10.1016/j.envpol.2016.11.005.

Zhang, H., Pap, S., Taggart, M.A., Boyd, K.G., James, N.A., Gibb, S.W., 2019. A review of the potential utilisation of plastic waste as adsorbent for removal of hazardous priority contaminants from aqueous environments. Environ. Pollut., 113698 https://doi.org/10.1016/j.envpol.2019.113698.

Zhang, J., Chen, H., He, H., Cheng, X., Ma, T., Hu, J., Yang, S., Li, S., Zhang, L., 2020. Adsorption behavior and mechanism of 9-Nitroanthracene on typical microplastics in aqueous solutions. Chemosphere 245, 125628. https://doi.org/10.1016/j.chemosphere.2019.125628.

Zhao, L., Rong, L., Xu, J., Lian, J., Wang, L., Sun, H., 2020. Sorption of five organic compounds by polar and nonpolar microplastics. Chemosphere 257, 127206. https://doi.org/10.1016/j.chemosphere.2020.127206.

Zuo, L.Z., Li, H.X., Lin, L., Sun, Y.X., Diao, Z.H., Liu, S., Zhang, Z.Y., Xu, X.R., 2019. Sorption and desorption of phenanthrene on biodegradable poly(butylene adipate co-terephtalate) microplastics. Chemosphere 215, 25–32. https://doi.org/10.1016/j.chemosphere.2018.09.173.